Supplemental Information

for

pH Responsive Polymer Cushions for Probing Membrane Environment Interactions

Rita J. El-khouri[^], Daniel A. Bricarello[#], Erik B. Watkins[*], Caroline Y. Kim[‡], Chad E. Miller[†], Timothy E. Patten[^], Atul N. Parikh[#], Tonya L. Kuhl[‡,¶]

Materials. Chloroform solutions of high-purity 1, 2 dipalmitoyl-sn-glycerol-3-phosphocholine (10 mg/ml, DPPC), 1,2-dimyristoleoyl-sn-glycero-3-phosphocholine (DMPC), 1-palmitoyl-2-oleoyl-sn-glycero-3-phosphocholine (POPC), and Texas Red® 1,2-dihexadecanoyl-sn-glycero-3-phosphoethanolamine, triethylammonium salt (1 mg/ml, TR-DHPE) were purchased from Avanti Polar lipids (Alabaster, AL) and Invitrogen (Carlsbad , CA) respectively. Poly(acrylic acid) (PAA, MW 450k g/mol, 0.1% crosslinked) and aminopropyltriethoxysilane (APTES) were purchased from Aldrich (St. Louis, MO) and used without further purification.

Experimental Methods

Preparation of PAA coated Surfaces. Prior to poly(acrylic acid) (PAA) deposition, all glass microscope slips, silica wafers, and quartz substrates were cleaned using the following procedure to remove organics and create surface silanols. First, the substrates were sonicated in MilliQ deionized water and optical soap for ten minutes. The surfaces were generously rinsed with MilliQ deionized water, and then sonicated for an additional ten minutes in isopropanol. A final sonication in acetone and subsequently isopropanol was conducted before the samples were again rinsed in

MilliQ deionized water and dried under a stream of Nitrogen (N_2). Finally, the substrates were placed in a UV-Ozone chamber for 30-40 min. The samples were water wetting, contact angle <10º as characterized via contact angle measurements.

The treated substrates were then immersed for 1 h in a gently stirred solution of APTES:toluene (~1 mMol). Samples were then rinsed in fresh toluene, quickly dried under a stream of clean N_2 and cured at 100 °C for 2 h. At the end of the curing process, the samples were removed from the oven and allowed to cool to room temperature. The average measured contact angle for these samples was 48-52°, and the average ellipsometric thickness was ~2 nm.

Poly(acrylic acid) (PAA) (450k MW, 0.1% cross-linked) was then deposited using the following spin coating technique. Three different concentrations of PAA in methanol were used: 1, 2, or 5 mg/mL. Solutions were stirred for 16 h, following 15 min of sonication. Prior to spin coating, the solutions were filtered through a 0.2 micron Whatman® PFTE filter. A 10-50 µL drop, volume based on substrate size, of solution was placed onto the substrate, and the sample was spin-coated at 2000 RPM for 120 s. Upon completion, the sample was cured to promote covalent linkage between the PAA and the APTES through amide formation or rinsed with MilliQ deionized water in order to remove excess PAA. If cured, samples were soaked in pH 8-10 water to convert any anhydrides formed back to carboxylates. Contact angle, AFM, and Ellipsometry are used to characterize these samples.
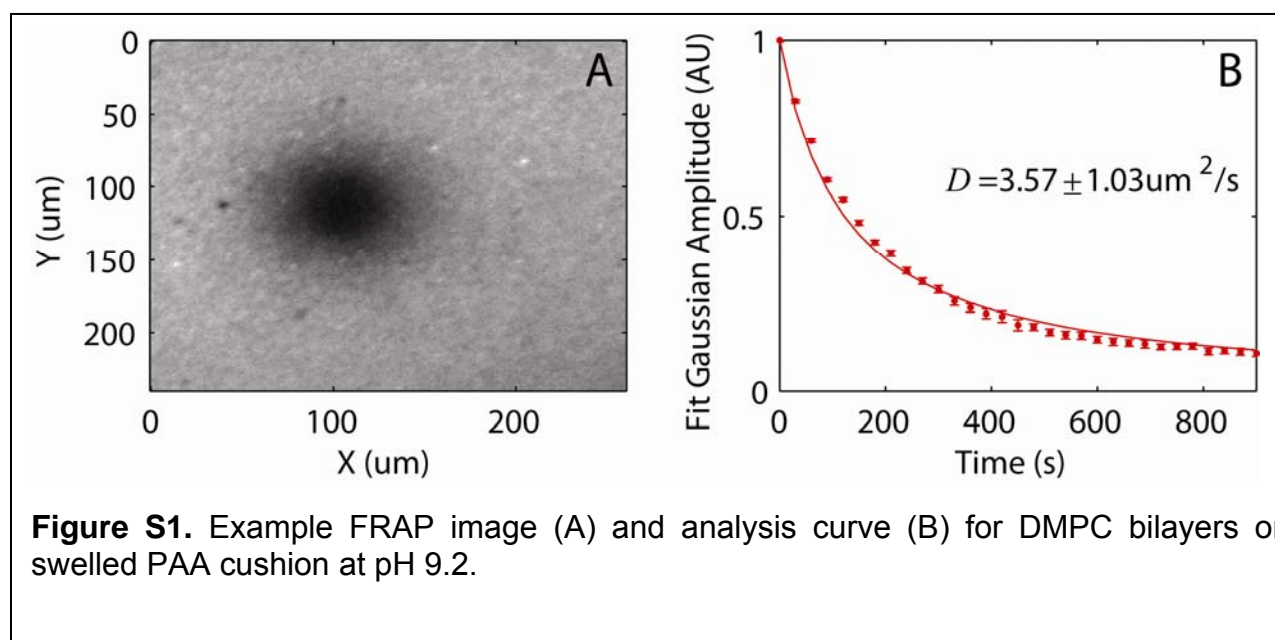
Langmuir Blodgette/Langmuir Schaefer (LB/LS) Membrane Deposition. First, a PAA coated substrate was submerged into the pH = 4 subphase (adjusted using 0.1M HCl or acetic acid/sodium acetate buffer 100mM) at room temperatue, ~25°C. Spreading solutions were 1mg/ml lipid-chloroform solution and 30 min was allowed for evaporation prior to compression of the desired lipid monolayer. Once the set surface pressure was attained, typically 30-45mN/m, the monolayer was left to equilibrate at this surface pressure for at least 10 min. Afterwards, the submerged substrate was slowly removed from the air-water interface at a rate of 1 mm/s. Once the substrate was fully removed from the subphase, the top leaflet was deposited using Langmuir Schaefer (LS) technique where the substrate was stamped through the interface in a horizontal configuration to yield a PAA cushioned membrane bilayer. Similar results were also obtained when the subphase was simply MilliQ deionized water (pH ~5.8).

Fluorescence Recovery After Photobleaching (FRAP). All FRAP measurements were conducted on a Nikon Eclipse TE2000-S inverted fluorescence microscope (Technical Instruments, Burlingame, CA) equipped with an ORCA-ER (model LB10-232, Hamamatsu Corp., Bridgewater, NJ) or Retige-1300 CCD camera (Technical Instruments). An Hg lamp as the light source was used to visualize all fluorescent samples. Two filter wheels, one containing a set of excitation filters and the other emission filters, were mounted in front of the light source and the CCD camera, respectively. An extra triple-band emitter was installed in the dichroic mirror cube for aiding in focusing through the eyepiece. Typically, images were taken using either a Plan Fluor 10× (NA, 0.25) or a Plan Fluor, ELWD, 20× (NA 0.45) objective (Nikon, Japan). High-resolution images were obtained using 100× (NA 1.4) oil-immersion

objectives. Images were stored and processed using simple PCI software (Compix, Inc., Cranberry Township, PA) augmented with a quantitative dynamic intensity analysis module.
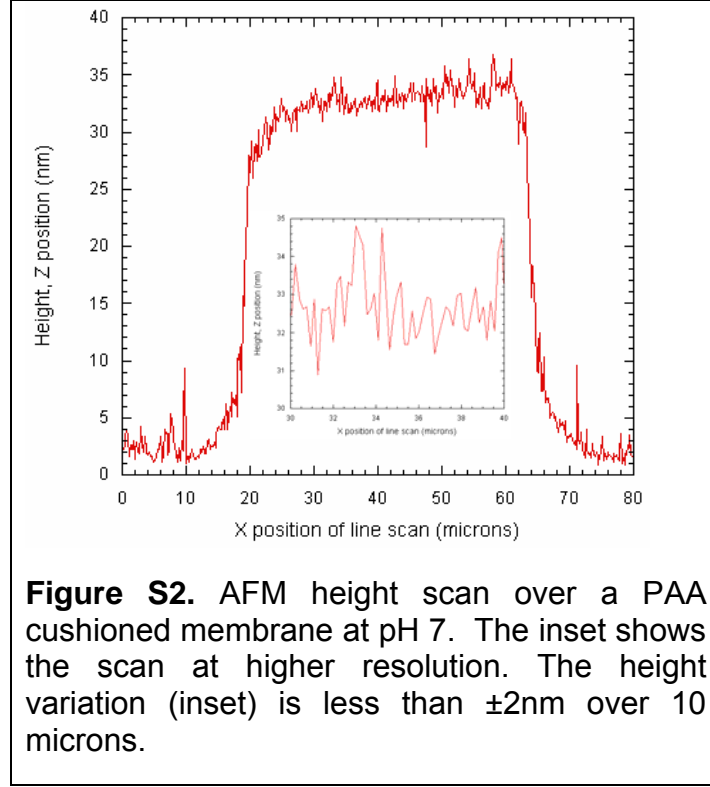
A typical FRAP measurement entailed continuous high power illumination (at the excitation wavelength of the fluorophore used) over a 30-50µm circular region on the fluorescent sample for 2 min. Such exposure results in a bleached dark spot on the sample. Following bleaching the excitation pathway was replaced with a low-power observation beam through a 10x objective in order to record wide-field images of the fluorescent recovery process.   Images were collected every 2, 5, 10, or 30 seconds and then processed to calculate diffusion coefficients (D) [1]. At pH 4 almost no recovery was observed.

The obtained video was processed using a FRAP analysis algorithm created in MATLAB (MathWorks, Natick MA) in the Parikh research team and is further described in detail elsewhere [2]. Briefly, for each frame collected of the bleached spot, the location was determined and its intensity cross-sectional profile was fit. Using the standard diffusion equation with Gaussian initial conditions produces a time-evolving Gaussian, and the spreading of the bleach spot can be fit as a function of time. A diffusion coefficient is extracted from the obtained Gaussian amplitude vs. time curve. A typical example image and intensity curve used to determine the diffusivity are shown in **Figure S1**.

Figure S1. Example FRAP image (A) and analysis curve (B) for DMPC bilayers on swelled PAA cushion at pH 9.2.

Atomic Force Microscopy. Atomic Force Microscopy (AFM) was conducted using a Dimension 3100 Scanning Probe Microscope with a Hybrid closed-loop XYZ head and Nanoscope IV a controller (Vecco, Santa Barbara, CA). All samples were imaged while submerged in fluid of the desired pH with a direct drive cantilever holder for fluids (Vecco, Santa Barbara, CA) at room temperature. A silicon nitride cantilever with a spring constant of 0.05 N/m was used to produce tapping mode scans at a scan rate of

0.5 Hz. Solution pH was monitored continuously and adjusted to maintain the desired pH with HCl or NaOH solutions. **Figure S2** shows an example higher resolution line scan plot for the data shown in **Figure S2** of the text. The bilayer is conformal, as evidenced by fluorescence microscopy measurements, and follows the height variations of the PAA cushion.

Figure S2. AFM height scan over a PAA cushioned membrane at pH 7. The inset shows the scan at higher resolution. The height variation (inset) is less than ±2nm over 10 microns.

Neutron and X-ray Reflectivity. Reflectivity, R, is defined as the ratio of the number of particles (neutrons or photons) elastically and specularly scattered from a surface to that of th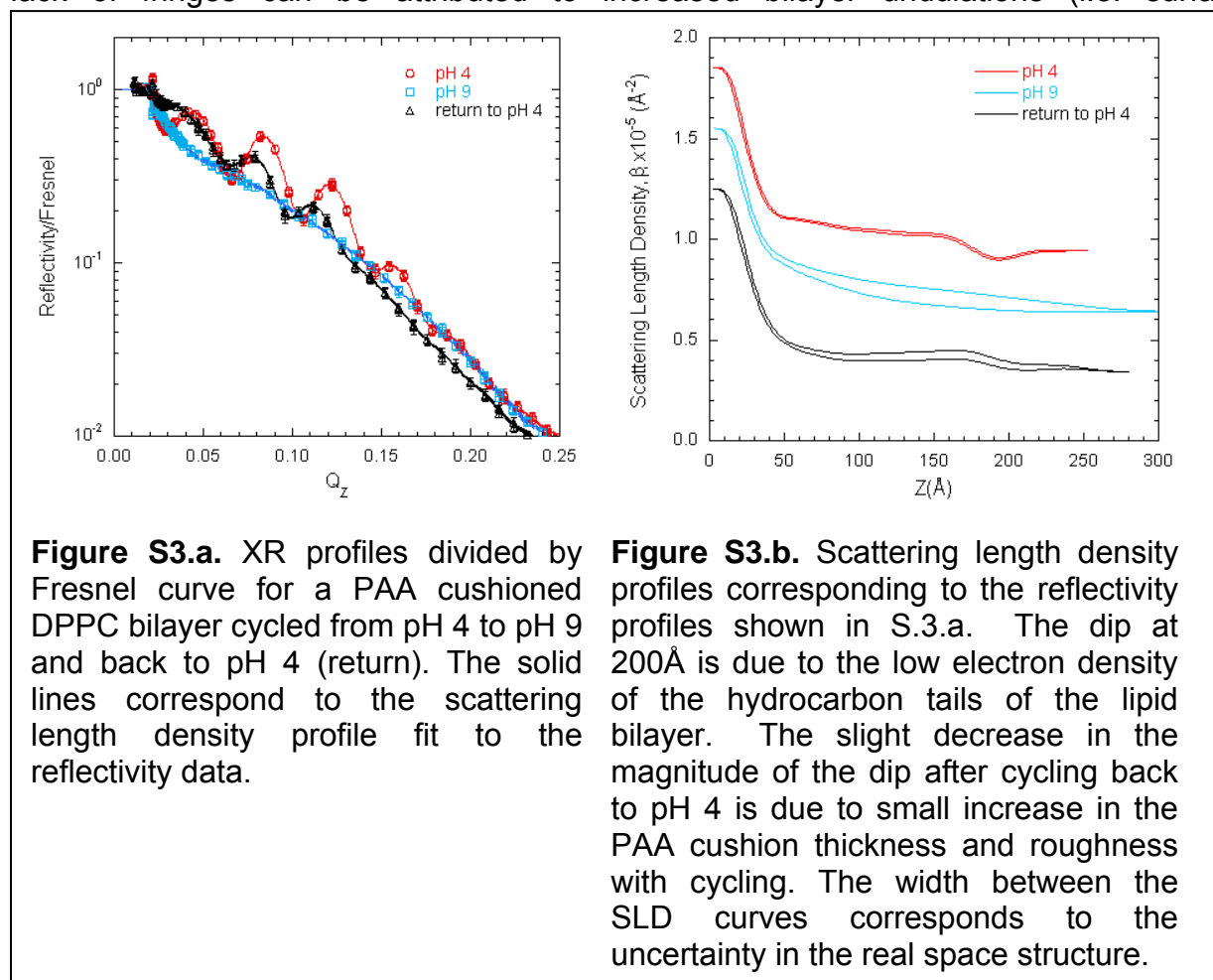e incident beam. When measured as a function of wave-vector transfer, $Q_Z = |k_{out} - k_{in}| = \dfrac{4\pi \sin \theta}{\lambda}$, where θ is the angle of incidence and λ is the wavelength of the beam), the reflectivity curve contains information regarding the sample-normal profile of the in-plane averaged scattering length density (SLD) and is therefore most suited for studies of interfacial, layered films. From the measured reflectivity profile, the thickness, SLD, and roughness of a series of layers normal to the substrate can be determined by minimizing the difference between the measured reflectivity and that obtained from a modeled SLD profile [5].

Neutron reflectivity (NR) experiments were performed on the SPEAR beamline at the Manuel Lujan Neutron Scattering Center (Los Alamos National Laboratory). Neutron reflectivities down to $R \approx 1\times10^{-6}$, and momentum transfers out to $Q_z,= \sim 0.25Å^{-1}$ are measured   The uncertainty of the Q_z resolution, $\sigma Q_z/Q_z$, including instrumental resolution was approximately 3% for the entire range of scattering vectors. X-ray

reflectivity (XR) measurements were carried out at beamline 6-ID at the Advanced Photon Source (Argonne National Laboratory) at λ = 0.545Å, which enabled measurements through a 1cm thick water layer [3,4]. The footprint of the x-ray beam on the sample was ~1x10 mm. High photon flux, relative to the much lower neutron flux, allowed high resolution XR measurements up to Q_z = 0.8Å^{-1}. An acetic acid/sodium acetate buffer was used to maintain a pH of 4. A phosphate buffer was used to maintain a pH of 9. Measurements were done at room temperature that varied from 24-28°C with DPPC membranes deposited at 45mN/m using LB/LS.

In addition to neutron reflectivity measurements, the formation of a single, PAA cushioned, DPPC membrane was also verified by X-ray reflectivity (XR). The structural reproducibility of the cushioned membrane system following swelling at elevated pH is also demonstrated by our X-ray reflectivity results. In the reflectivity divided by Fresnel curves (**Figure S3.a**), interference fringes are observed at pH 4 both before and after swelling the PAA cushion. These fringes result from the electron density contrast provided by the low density membrane supported by the hydrated polymer cushion. Fringes are no longer visible when the polymer is swelled in a pH 9 aqueous solution. However, since fringes return when the pH is subsequently lowered to pH 4, the absence of fringes at pH 9 does not indicate a removal of the lipid bilayer. Instead, the lack of fringes can be attributed to increased bilayer undulations (i.e. surface

Figure S3.a. XR profiles divided by Fresnel curve for a PAA cushioned DPPC bilayer cycled from pH 4 to pH 9 and back to pH 4 (return). The solid lines correspond to the scattering length density profile fit to the reflectivity data.

Figure S3.b. Scattering length density profiles corresponding to the reflectivity profiles shown in S.3.a. The dip at 200Å is due to the low electron density of the hydrocarbon tails of the lipid bilayer. The slight decrease in the magnitude of the dip after cycling back to pH 4 is due to small increase in the PAA cushion thickness and roughness with cycling. The width between the SLD curves corresponds to the uncertainty in the real space structure.

roughness) which interfere destructively or a swelled cushion thickness beyond the instrumental resolution.

To extract more precise structural information, the reflectivity data was analyzed to obtain the electron density profile normal to the interface, $\beta(z)$. using a model-free approach based on cubic B-splines. We performed over a thousand refinements within the parameter space and present a family of models for each reflectivity data set, all of which satisfy $\chi^2 \leq \chi^2_{min}+1$ [4,6]. The superposition of the profiles yields an electron density "band" which is a measure of the uncertainty in the real space structure (**Figure S3b** – region between lines). In terms of the fitted electron density profiles, at pH 4, the membrane's presence is indicated by a low electron density region approximately 200Å from the solid support. This feature of the SLD profile is completely absent at pH 9 and returns when the pH is lowered to 4. The electron density dip corresponding to the cushioned membrane is slightly less visible following swelling and re-collapsing the polymer cushion. This decreased visibility of the bilayer is most likely due to a modest increase in disorder of the polymer cushion structure upon re-collapse.

Imaging Ellipsometry. Ellipsometric angles and spatially resolved ellipsometric contrast images were acquired using a commercial Elli2000 imaging system (Nanofilm Technologie, Göttingen, Germany). The ellipsometer employed a frequency-doubled Nd:YAG laser (adjustable power up to 20 mW) at 532 nm and was equipped with a motorized goniometer for an accurate selection of the incidence angle and corresponding detector positions. The ellipsometer employed the typical polarizer-compensator-sample-analyzer (PCSA) nulling configuration in which a linear polarizer (P) and a quarter-wave plate (C) yield an elliptically polarized incident beam. On reflection from the sample (S), the beam was gathered via an analyzer (A) and imaged onto a CCD camera through a long-working-distance 10× objective. The P, C, and A positions that yielded the null condition were then converted to the ellipsometric angles, Δ and Ψ. Measurements were generally taken at an incidence angle of 60°. Silicon substrates with native oxide overlayer (SiO$_2$/Si) whose surface chemistry was comparable to that of glass were used to enhance the optical contrast with the lipid phase. For characterization under aqueous conditions, a fluid cell was used (Nanofilm Technologie, Göttingen, Germany). The cell consisted of a Teflon chamber (3 ml volume) with glass windows fixed at 60° (incidence angle) to the substrate normal. The field of view and lateral resolution of the acquired images were limited by the objective and CCD used. The specified accuracy in ellipsometric angle determination is 0.01° for this instrument.

Contact Angle. Contact angle measurements were conducted on a VCA optima instrument (AST products inc., Billerica, MA), which was equipped with a CCD camera to capture static or movie images. An automatic syringe was used to dispense a 0.75 µL MilliQ deionized water droplet onto the substrate. The instrument was equipped with AutoFAST imaging software, which traced the shape of the droplet and calculated the advancing contact angle by sessile drop method.

S6

W-31-109-Eng-38.

[1] Yee, C. K., Amweg, M. L., and Parikh A. Direct Photochemical Patterning and Refunctionalization of Supported Phospholipid Bilayers, J. Am. Chem. Soc., 2004, 126(43), 13962–13972.

[2] B. Sanii, A.M. Smith, R. Butti, A.M. Brozell, and A.N. Parikh Nano Lett., 2008, 8 (3), pp 866–871 DOI: 10.1021/nl073085b

[3] Miller, C. E., Majewski, J., Watkins, E. B., Mulder, D. J., Gog, T., and Kuhl, T. L. "Probing the local order of single phospholipid membranes using grazing incidence x-ray diffraction," Phys. Rev. Lett. 100, 058103 (2008).

[4] Watkins, E.B., Miller, C.E., Mulder, D.J., Kuhl, T.L., and Majewski, J. "Structure and orientational texture of self-organizing lipid bilayers," Phys. Rev. Lett. 102(23) 4 (2009).

[5] Kjaer, K. 1994. Some Simple Ideas on X-Ray Reflection and Grazing-Incidence Diffraction from Thin Surfactant Films. Physica B 198:100-109.

[6] J. S. Pedersen, and I. W. Hamley, Physica B **198**, 16 (1994).